JOURNAL OF THEORETICAL AND APPLIED MECHANICS
56, 4, pp. 1123-1137, Warsaw 2018
DOI: 10.15632/jtam-pl.56.4.1123

AN EFFICIENT ANALYSIS OF STEADY-STATE HEAT CONDUCTION INVOLVING CURVED LINE/SURFACE HEAT SOURCES IN TWO/THREE-DIMENSIONAL ISOTROPIC MEDIA

Mehrdad Mohammadi
Department of Mechanical Engineering, Shiraz Branch, Islamic Azad University, Shiraz, Iran

Mohammad R. Hematiyan
Department of Mechanical Engineering, Shiraz University, Shiraz, Iran

Yuichuin C. Shiah
Department of Aeronautics and Astronautics, National Cheng Kung University, Tainan, Taiwan, R.O.C.
e-mail: ycshiah@mail.ncku.edu.tw

In this paper, a new formulation based on the method of fundamental solutions for two/three-dimensional steady-state heat conduction problems involving internal curved line/surface heat sources is presented. Arbitrary shapes and non-uniform intensities of the curved heat sources can be modeled by an assemblage of several parts with quadratic variations. The presented mesh-free modeling does not require any internal points as in domain methods. Four numerical examples are studied to verify the validity and efficiency of the proposed method. Our analyses have shown that the presented mesh-free formulation is very efficient in comparison with conventional boundary or domain solution techniques.

Keywords: heat conduction, concentrated heat source, curved heat source, mesh-free method

1. Introduction

Heat conduction and thermoelasticity involving boundary or domain heat sources have been subject of many studies in the last years, and they are still active areas of researches (e.g. Rogowski, 2016; Hidayat *et al.*, 2017). In real applications, it is quite often to have internal heat sources concentrated on points, lines or curved paths due to electrical heating or some other heat sources like laser beams. As examples, we can mention infrared heating, a method of electric heating that is frequently used in the metallurgy and textile industries, laser beam heating/welding that is used in automotive and aerospace industries, and friction heating for material processing and joining. Despite several analytical solutions for simple problems involving concentrated heat sources (e.g. Chao and Tan, 2000; Han and Hasebe, 2002), practical problems with complicated conditions still need to resort to numerical tools. The accuracy analysis of the domain solution methods such as the finite element method (FEM) depends on the mesh density especially near the concentrated heat source. As powerful alternative approaches, the boundary methods such as the boundary element method (BEM) and the method of fundamental solutions (MFS) only require boundary discretization.

To date, the BEM has been effectively used to solve direct and inverse problems containing concentrated sources of heat generation. Le Niliot (1998) proposed a boundary element formulation for identification of the intensity of point heat sources in diffusive systems. In another work, Le Niliot and Lefèvre (2001) proposed a BEM to identify the location and strength of multiple point heat sources in a transient heat conduction problem. Karami and Hematiyan (2000a,b) proposed a formulation based on the BEM for direct and inverse analyses of heat conduction problems containing concentrated sources of heat generation. They presented an exact implementation of a source of heat generation concentrated on a point or a line in the BEM formulation. Shiah *et al.* (2005) analyzed two-dimensional thermo-mechanical problems containing point sources using the BEM. They could solve the problem with boundary-only discretization. In another research, Shiah *et al.* (2006) used the direct domain mapping (DDM) technique to analyze 2D and 3D heat conduction problems in composites consisting of multiple anisotropic media with embedded point heat sources. Hematiyan *et al.* (2011) presented a formulation based on the BEM for analysis of two and three dimensional thermo-elastic problems involving point, line and area heat sources. They only employed boundary discretization in their formulation. However, their proposed formulation considered only straight line and flat surface heat sources with a linear variation of the heat source intensity. Mohammadi *et al.* (2016) used the BEM for analysis of two- and three-dimensional thermo-elastic problems involving arbitrary curved line heat sources. They effectively solved the problem without considering any internal points/cells; but they did not consider curved surface heat sources.

The present work uses the MFS to analyze problems of 2D/3D heat conduction involving internal concentrated heat sources. In this paper, the MFS, a widely applied meshless method, is shown to be very efficient for the analysis on account of which the benefit is that no internal points/nodes are required for the modeling. Similar to the BEM, the MFS is applicable when a fundamental solution of the problem is known. However, the important advantage of the MFS over the BEM is that the MFS is an integration-free method and it can be easily implemented for problems especially in three-dimensional and irregular domains. The basic idea of the MFS is to approximate the solution as a linear combination of fundamental solutions. The singularities (sources) of the fundamental solutions are located outside the physical domain of the problem. The MFS solutions exactly satisfy governing equations of the problem and approximately satisfy boundary conditions. In the study carried out by Fairweather and Karageorghis (1998), the development of the MFS in the past three decades was explained.

The equation governing steady-state heat conduction in a medium with a heat source is the standard Poisson equation. To solve Poisson's equation using the MFS, a particular solution corresponding to the heat source term in addition to a homogeneous solution of the Laplace equation should be found. Two important methods proposed to calculate this particular solution are the Atkinson method (1985) and the dual reciprocity method (DRM) (Partridge *et al.*, 1992). In Atkinson's method, the particular solution is taken to be a Newton potential and is obtained by evaluating a domain integral. Poullikkas *et al.* (1998) used this method for solving inhomogeneous harmonic and biharmonic problems. In the DRM, the particular solution is approximated by a series of basis solutions. As an example, Golberg (1995) used this method to solve Poisson's equation without a boundary or domain discretization.

In this work, the MFS is formulated for 2D/3D problems of heat conduction involving internal heat sources concentrated on curved lines/surfaces. Although the MFS has been widely used for analysis of heat conduction problems in different conditions (e.g. Ahmadabadi *et al.*, 2009; Kołodziej *et al.*, 2010; Mierzwiczak and Kołodziej, 2012); however, to the authors' knowledge, the MFS formulation for analysis of internal curve line/surface heat sources has not been presented yet. The method presented here can be simply employed without considering any internal points/nodes and, therefore, it preserves the attractiveness of the MFS as a boundary--type mesh-free method. Several two- and three-dimensional numerical examples are presented at the end to show that the proposed formulation is very efficient to yield accurate results in comparison with the BEM and FEM.

2. MFS formulation for steady-state heat conduction in a domain including heat sources

Consider an isotropic medium Ω with its boundary Γ (Fig. 1). In the presence of heat sources, the governing equation of steady-state heat conduction can be expressed as follows

$$\nabla^2\tau(\mathbf{x}) = -\frac{s(\mathbf{x})}{k} \qquad \mathbf{x} \in \Omega \tag{2.1}$$

where ∇^2 represents the Laplace operator, τ is temperature, k is thermal conductivity, and $s(\mathbf{x})$ is a known function describing the heat source distribution.

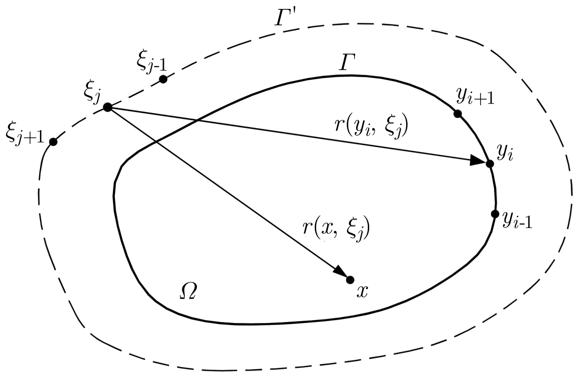

Fig. 1. Domain Ω, boundary Γ and pseudo boundary Γ'

Boundary condition in a generalized form can be written as follows

$$f_1\tau + f_2\frac{\partial\tau}{\partial n} = f_3 \qquad \text{on} \quad \Gamma \tag{2.2}$$

where f_1, f_2 and f_3 are given functions on the boundary and n is the normal direction.

In the MFS, the solution to Poisson equation (2.1) is approximated by a linear combination of fundamental solutions of the Laplace equation and a particular solution

$$\tau(\mathbf{x}) = \sum_{j=1}^{N} a_j\tau^*(\mathbf{x},\boldsymbol{\xi}_j) + \tau_p(\mathbf{x}) \tag{2.3}$$

where $\boldsymbol{\xi}_j$ and a_j are the known location and unknown intensity of the j-th source located on the pseudo-boundary Γ' (Fig. 1), respectively. $\mathbf{x}$ is a point in the domain or on the boundary of the solution domain, and N is the number of sources. τ^* represents the fundamental solution to the Laplace operator that is given as follows

$$\tau^*(\mathbf{x},\boldsymbol{\xi}_j) = \begin{cases} \dfrac{-1}{2\pi}\ln(r(\mathbf{x},\boldsymbol{\xi}_j)) & \text{for} \quad 2D \\ \dfrac{1}{4\pi r(\mathbf{x},\boldsymbol{\xi}_j)} & \text{for} \quad 3D \end{cases} \tag{2.4}$$

where $r(\mathbf{x},\boldsymbol{\xi}_j)$ is the distance between the field point $\mathbf{x}$ and the source point $\boldsymbol{\xi}_j$. $\tau_p(\mathbf{x})$ is the particular solution to equation (2.1) associated to the heat source function $s(\mathbf{x})$ that can be concentrated on a part of the domain or distributed over the entire domain. The particular solution can be obtained by constructing the associated Newton potential in the following domain integral form

$$\tau_p(\mathbf{x}) = \frac{1}{k}\int\limits_{\Omega} s(\boldsymbol{\xi})\tau^*(\mathbf{x},\boldsymbol{\xi})\ dV(\boldsymbol{\xi}) \tag{2.5}$$

Efficient evaluation of this domain integral is very important in the MFS to maintain the attractiveness of the method. If one can evaluate the domain integral in Eq. (2.5) without considering any internal cells/points, the attractiveness of the MFS is preserved.

The constants a_j (with the unit m°C in the SI system) are unknown intensities of the sources and they have to be found. To find these unknowns, we consider N boundary points $\mathbf{y}_1, \mathbf{y}_2, \ldots, \mathbf{y}_N$ that are a priori located on Γ and collocate the corresponding boundary condition at these points. From Eqs. (2.2) and (2.3), the following equation is obtained

$$\begin{aligned}\sum_{j=1}^{N} a_j \Big[f_1(\mathbf{y}_i)\tau^*(\mathbf{y}_i, \boldsymbol{\xi}_j) + f_2(\mathbf{y}_i)\frac{\partial \tau^*(\mathbf{y}_i, \boldsymbol{\xi}_j)}{\partial n}\Big] &= f_3(\mathbf{y}_i) \\ - \Big[f_1(\mathbf{y}_i)\tau_p(\mathbf{y}_i) + f_2(\mathbf{y}_i)\frac{\partial \tau_p(\mathbf{y}_i)}{\partial n}\Big] & \qquad i = 1, 2, \ldots, N\end{aligned} \tag{2.6}$$

which represents a system of N linear equations with N unknowns. In general, one can write system (2.6) as follows

$$\mathbf{AX} = \mathbf{F} \tag{2.7}$$

where the components of the matrix $\mathbf{A} \in \mathcal{R}^{N\times N}$ and the vectors $\mathbf{F} \in \mathcal{R}^N$ and $\mathbf{X} \in \mathcal{R}^N$ are expressed as follows

$$\begin{aligned}A_{ij} &= f_1(\mathbf{y}_i)\tau^*(\mathbf{y}_i, \boldsymbol{\xi}_j) + f_2(\mathbf{y}_i)\frac{\partial \tau^*(\mathbf{y}_i, \boldsymbol{\xi}_j)}{\partial n} \\ F_i &= f_3(\mathbf{y}_i) - \Big[f_1(\mathbf{y}_i)\tau_p(\mathbf{y}_i) + f_2(\mathbf{y}_i)\frac{\partial \tau_p(\mathbf{y}_i)}{\partial n}\Big] \qquad X_i = a_i\end{aligned} \tag{2.8}$$

By selecting a suitable configuration for boundary and source points, Eq. (2.7) can be solved by standard methods such as the Gaussian elimination method.

In the next Section, the method for computation of the particular solution $\tau_p(\mathbf{x})$ using Eq. (2.5) for the special case of heat sources concentrated on a curved line/surface is described.

3. Formulations for heat sources concentrated on a curved line/surface

In this Section, particular solutions associated to curved line/surface heat sources in the MFS are presented. For the 2D case, curved line sources, while for the 3D case, both curved line and curved surface sources are considered.

3.1. Curved line heat source in 2D problems

At first, the formulation for a curved line heat source with a quadratic shape is presented. It is also assumed that the intensity of the source has a quadratic variation along the heat source. An arbitrary curved line heat source can be modeled by several quadratic heat sources. A domain including a general curved line heat source and a part of the source modeled as a quadratic line heat source is illustrated in Fig. 2. Each quadratic line heat source is discretized by three points. The intensity per unit length of the source at the starting point (x_1, y_1), middle point (x_2, y_2), and end point (x_3, y_3) are represented by g_1, g_2, g_3, respectively.

Assuming a quadratic variation for the intensity of the heat source, $s(\mathbf{x})$ can be given as follows

$$s(\eta) = N_1 g_1 + N_2 g_2 + N_3 g_3 \tag{3.1}$$

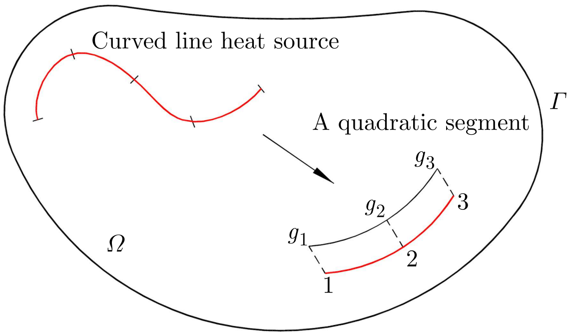

Fig. 2. An arbitrary curved line heat source modeled as several quadratic line heat sources

where the quadratic shape functions N_i are

$$N_1 = \frac{1}{2}\eta(\eta-1) \qquad N_2 = -(\eta+1)(\eta-1) \qquad N_3 = \frac{1}{2}\eta(\eta+1) \tag{3.2}$$

where η is a dimensionless local coordinate aligned with the quadratic segment that varies from -1 to 1.

Domain integral (2.5) for the quadratic line heat source can be expressed as follows

$$\tau_p(\mathbf{x}) = \int\limits_L \frac{s(\boldsymbol{\xi})}{k}\tau^*(\mathbf{x},\boldsymbol{\xi})\, dl \tag{3.3}$$

where dl is an infinitesimal element along the quadratic line heat source. Substituting τ^* in the 2D case from Eq. (2.4) into Eq. (3.3) results in

$$\tau_p(\mathbf{x}) = \frac{-1}{2\pi k}\int\limits_l s(\boldsymbol{\xi})\ln[r(\mathbf{x},\boldsymbol{\xi})]\, dl \tag{3.4}$$

where $r(\mathbf{x},\boldsymbol{\xi}) = \sqrt{(x-x_s)^2+(y-y_s)^2}$ is the distance between the field point $\mathbf{x}=(x,y)$ and the source points $\boldsymbol{\xi}=(x_s,y_s)$ on the quadratic line heat source. x_s and y_s can be expressed in terms of the three points of the quadratic line heat source as follows

$$x_s = (N_1x_1+N_2x_2+N_3x_3) \qquad y_s = (N_1y_1+N_2y_2+N_3y_3) \tag{3.5}$$

Using Eqs. (3.5), the infinitesimal element dl in Eq. (3.4) can be expressed as

$$dl = \sqrt{dx_s^2+dy_s^2} = J\,d\eta \tag{3.6}$$

where J is Jacobian which can be expressed as

$$J = \sqrt{\Big(x_1\frac{dN_1}{d\eta}+x_2\frac{dN_2}{d\eta}+x_3\frac{dN_3}{d\eta}\Big)^2+\Big(y_1\frac{dN_1}{d\eta}+y_2\frac{dN_2}{d\eta}+\mathbf{y}_3\frac{dN_3}{d\eta}\Big)^2} \tag{3.7}$$

Substituting Eqs. (3.1) and (3.6) into Eq. (3.4) results in

$$\tau_p(\mathbf{x}) = \frac{-1}{2\pi k}\int\limits_{-1}^{1}(N_1g_1+N_2g_2+N_3g_3)\ln[r(\eta)]J\,d\eta \tag{3.8}$$

The integral in Eq. (3.8) can be calculated using conventional numerical integration methods such as the Gaussian quadrature method (GQM). It should be noted that if the field point

$\mathbf{x} = (x, y)$ is exactly on the line source, the integral in Eq. (3.8) will be weakly singular with a finite value. In other words, in the two-dimensional case, the temperature has a finite value at points exactly on the curved line heat source. In this case, the integral in Eq. (3.8) can be calculated by various methods such as the weighted Gaussian integration (Stroud and Secrest, 1996), transformation of variable (Telles, 1987) and subtraction of singularity (Aliabadi 2002) method. In this research, the weighted Gaussian integration method is used.

3.2. Curved line heat source in three-dimensional problems

Similar to 2D, the intensity per unit length of the quadratic line heat source at the starting point (x_1, y_1, z_1), middle point (x_2, y_2, z_2) and end point (x_3, y_3, z_3) are assumed g_1, g_2 and g_3, respectively.

Substituting τ^* in the 3D case from Eq. (2.4) into Eq. (3.3) results in

$$\tau_p(\mathbf{x}) = \frac{1}{4\pi k} \int_L \frac{s(\boldsymbol{\xi})}{r(\mathbf{x}, \boldsymbol{\xi})}\, dl \tag{3.9}$$

where $r(\mathbf{x}, \boldsymbol{\xi}) = \sqrt{(x - x_s)^2 + (y - y_s)^2 + (z - z_s)^2}$ is the distance between the field point $\mathbf{x} = (x, y, z)$ and the source point $\boldsymbol{\xi} = (x_s, y_s, z_s)$ on the line heat source. x_s, y_s, and z_s can be expressed as follows

$$\begin{aligned} &x_s = (N_1 x_1 + N_2 x_2 + N_3 x_3) \qquad && y_s = (N_1 y_1 + N_2 y_2 + N_3 y_3) \\ &z_s = (N_1 z_1 + N_2 z_2 + N_3 z_3) \end{aligned} \tag{3.10}$$

The infinitesimal element dl in Eq. (3.9) can be expressed as

$$dl = \sqrt{dx_s^2 + dy_s^2 + dz_s^2} = J\, d\eta \tag{3.11}$$

where

$$J = \sqrt{\left(\sum_{j=1}^{3} x_j \frac{dN_j}{d\eta}\right)^2 + \left(\sum_{j=1}^{3} y_j \frac{dN_j}{d\eta}\right)^2 + \left(\sum_{j=1}^{3} z_j \frac{dN_j}{d\eta}\right)^2} \tag{3.12}$$

Therefore, Eq. (3.9) can be written as follows

$$\tau_p(\mathbf{x}) = \frac{1}{4\pi k} \int_{-1}^{1} \frac{N_1 g_1 + N_2 g_2 + N_3 g_3}{r(\eta)} J\, d\eta \tag{3.13}$$

Similar to the 2D case, the integral in equation (3.13) can be evaluated using standard numerical integration methods such as the GQM. According to the integral in equation (3.13), it is clear that if the field point $\mathbf{x} = (x, y, z)$ is exactly on the curved line source, the integral in Eq. (3.13) will be a strongly singular integral without any finite value. In other words, in the 3D case, the temperature at points on the curved line source does not have a finite value.

3.3. Curved surface heat source in 3D problems

We consider a heat source distributed over a curved surface in a 3D domain. The shape of the surface source and its intensity function are assumed arbitrarily and sufficiently complicated. The surface of the heat source is discretized by several quadrilateral surfaces. Each quadrilateral surface heat source has a quadratic shape with a quadratic variation of the intensity over it.

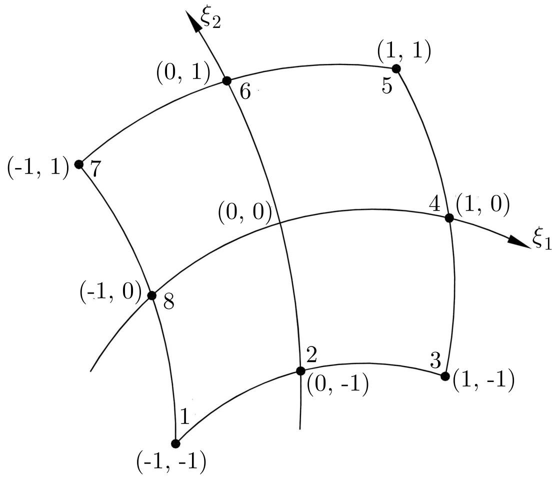

Fig. 3. A quadratic surface heat source

In this part, the formulation for treatment of a quadratic surface heat source is presented. A quadratic surface heat source, which is described by 8 points, is shown in Fig. 3.

The intensity per unit area of the quadratic surface heat source is written as follows

$$s(\xi_1,\xi_2) = \sum_{i=1}^{8} N_i(\xi_1,\xi_2) g_i \tag{3.14}$$

where $g_1, g_2, \ldots, g_8$ are the intensities per unit area at 8 points of the source, ξ_1 and ξ_2 are local coordinates which have a variation between -1 and 1 in the source. The shape functions N_i in terms of ξ_1 and ξ_2 are expressed as follows (Becker, 1992)

$$\begin{aligned}
N_1 &= \frac{-1}{4}(1-\xi_1)(1-\xi_2)(1+\xi_1+\xi_2) & N_2 &= \frac{1}{2}(1-\xi_1^2)(1-\xi_2)\\
N_3 &= \frac{-1}{4}(1+\xi_1)(1-\xi_2)(1-\xi_1+\xi_2) & N_4 &= \frac{1}{2}(1+\xi_1)(1-\xi_2^2)\\
N_5 &= \frac{-1}{4}(1+\xi_1)(1+\xi_2)(1-\xi_1-\xi_2) & N_6 &= \frac{1}{2}(1-\xi_1^2)(1+\xi_2)\\
N_7 &= \frac{-1}{4}(1-\xi_1)(1+\xi_2)(1+\xi_1-\xi_2) & N_8 &= \frac{1}{2}(1-\xi_1)(1-\xi_2^2)
\end{aligned} \tag{3.15}$$

The domain integral in Eq. (2.5) associated to the quadratic surface heat source is given as follows

$$\tau_p(\mathbf{x}) = \int\limits_A \frac{s(\boldsymbol{\xi})}{k} \tau^*(\mathbf{x},\boldsymbol{\xi})\, dA \tag{3.16}$$

where dA is an infinitesimal area element on the quadratic surface heat source. Substituting τ^* in the 3D case from Eq. (2.4) into Eq. (3.16) results in

$$\tau_p(\mathbf{x}) = \frac{1}{4\pi k} \int\limits_A \frac{s(\boldsymbol{\xi})}{r(\mathbf{x},\boldsymbol{\xi})}\, dA \tag{3.17}$$

where $r(\mathbf{x},\boldsymbol{\xi})$ is the distance between the field point $\mathbf{x} = (x,y,z)$ and the source points $\boldsymbol{\xi} = (x_s,y_s,z_s)$ on the quadratic surface heat source. x_s, y_s and z_s can be expressed in terms of the 8 shape functions as follows

$$x_s(\xi_1,\xi_2)=\sum_{i=1}^{8}N_i(\xi_1,\xi_2)x_i \qquad y_s(\xi_1,\xi_2)=\sum_{i=1}^{8}N_i(\xi_1,\xi_2)y_i$$
$$z_s(\xi_1,\xi_2)=\sum_{i=1}^{8}N_i(\xi_1,\xi_2)z_i \tag{3.18}$$

The infinitesimal area element dA can be written as follows (Becker, 1992)

$$dA=J(\xi_1,\xi_2)\,d\xi_1\,d\xi_2 \tag{3.19}$$

where

$$J=\sqrt{(J_x)^2+(J_y)^2+(J_z)^2} \tag{3.20}$$

and

$$J_x=\frac{\partial y_s}{\partial\xi_1}\frac{\partial z_s}{\partial\xi_2}-\frac{\partial z_s}{\partial\xi_1}\frac{\partial y_s}{\partial\xi_2} \qquad J_y=\frac{\partial z_s}{\partial\xi_1}\frac{\partial x_s}{\partial\xi_2}-\frac{\partial x_s}{\partial\xi_1}\frac{\partial z_s}{\partial\xi_2} \qquad J_z=\frac{\partial x_s}{\partial\xi_1}\frac{\partial y_s}{\partial\xi_2}-\frac{\partial y_s}{\partial\xi_1}\frac{\partial x_s}{\partial\xi_2} \tag{3.21}$$

Substituting Eqs. (3.19) and (3.14) into Eq. (3.17) results in

$$\tau_p(\mathbf{x})=\frac{1}{4\pi k}\int_{-1}^{1}\int_{-1}^{1}\frac{\sum_{i=1}^{8}N_i(\xi_1,\xi_2)g_i}{r(\xi_1,\xi_2)}J(\xi_1,\xi_2)\,d\xi_1\,d\xi_2 \tag{3.22}$$

The integral in Eq. (3.22) can be calculated using standard 2D numerical integration methods such as the GQM.

In the case that the field point $\mathbf{x}$ is exactly on the surface of the heat source, the integral in Eq. (3.22) will be weakly singular with a finite value. In other words, in the three-dimensional case, temperatures at points on a surface heat source have finite values. In this case, the integral in Eq. (3.22), which is weakly singular, can be calculated by various methods such as the transformation of variable and subtraction of singularity method (Aliabadi, 2002). In this research, the method of transformation of the variable is used for these cases.

4. Numerical examples

In this Section, two 2D and two 3D examples containing different kinds of curved heat sources are presented. In each example, the results computed by the presented MFS in comparison with the BEM and FEM are presented. Source codes are developed in MATLAB software for analysis of the examples using the MFS and BEM. ANSYS package is used for analysis of the examples using the FEM. The computations are implemented on a laptop with an Intel(R) (Intel, Inc., Santa Clara, CA, USA) Core(TM) i7-2670QM CPU of 2.20 GHz, on 64-bit Windows operating system with 8.00 GB RAM. In all examples, the thermal conductivity is $k = 60\,\mathrm{W/(m^\circ C)}$.

4.1. A circular domain including a circular heat source

In this example, according to Fig. 4, a circular domain with $R = 0.5$ is considered. This problem is analyzed under the Dirichlet boundary condition with $\tau_B = 10^\circ\mathrm{C}$. A curved heat source which is distributed over a circle with the radius $r = 0.25\,\mathrm{m}$ is considered. The strength of the heat source is considered to be constant over the circle and equal to $s = 4000\,\mathrm{W/m}$. The pseudo boundary Γ' is considered to be a circle with radius $R' = 2.5\,\mathrm{m}$ (5 times of R). Only

4 sources are considered on this pseudo-boundary. The circular heat source is modeled by only four quadratic line heat sources. The obtained results by the proposed MFS are compared with those of the BEM (32 linear boundary elements) and FEM (9461 quadratic elements) presented in (Mohammadi *et al.*, 2016). The temperature results along the vertical diameter of the circle are shown in Fig. 5. As can be seen, the presented MFS formulation yields very accurate results.

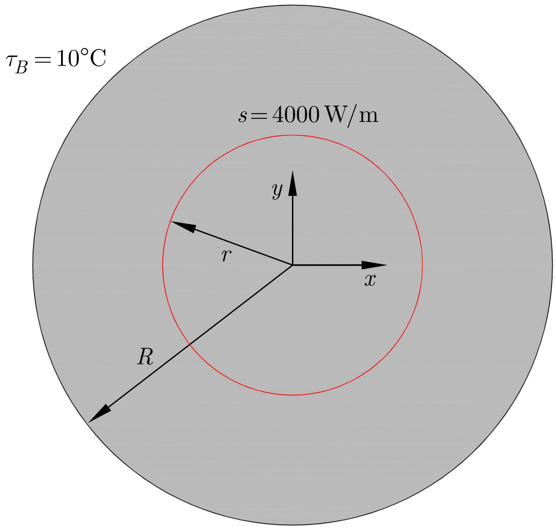

Fig. 4. A circular domain including a circular heat source

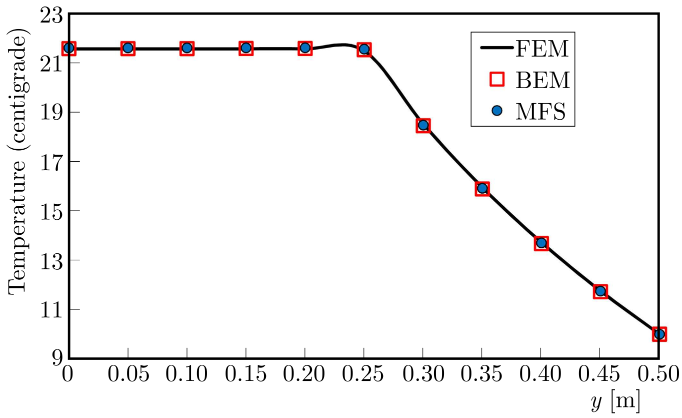

Fig. 5. Temperature on the vertical diameter (y-axis) of the circle obtained by the FEM, BEM and MFS

4.2. A rectangular domain including a heat source with an elliptical shape and non-uniform intensity

In this example, a heat conduction problem over a 0.15×0.3 m rectangle containing a curved heat source is considered. Figure 6a shows the geometry and thermal boundary conditions of the problem.

An elliptical curved line heat source centered at $(0.085, 0.065)$ is considered in the domain. The lengths of the horizontal and vertical radii of the ellipse are $r_1 = 0.04$ m and $r_2 = 0.02$ m, respectively. The heat source intensity is considered to be a function of $\beta \in [0, 2\pi]$ as follows

$$s = 40000(1 + \cos\beta)\ \mathrm{W/m} \tag{4.1}$$

where β is the angular coordinate on the heat source measured from a horizontal axis passing through the center of the ellipse (Fig. 6a).

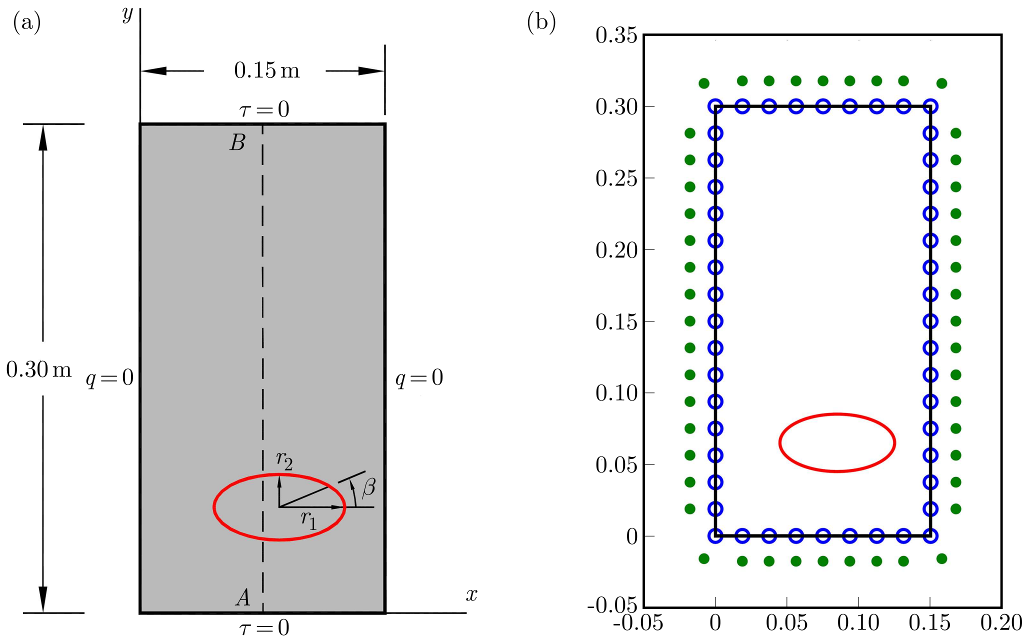

Fig. 6. A rectangle with an elliptical heat source: (a) geometry and boundary conditions, (b) configuration of collocation and source points

In the proposed MFS, the elliptical heat source is modeled by only eight quadratic heat sources. 48 source points and 48 collocation points are considered for the MFS analysis. The configuration of collocation and source points is depicted in Fig. 6b. The locations of source points are determined according to the method suggested by Hematiyan *et al.* (2018). The ratio of the distance from the source point to its corresponding collocation point to the distance from the same source point to the neighboring collocation point is 0.85. By this configuration, a solution without undesired oscillation is obtained (Hematiyan *et al.*, 2018).

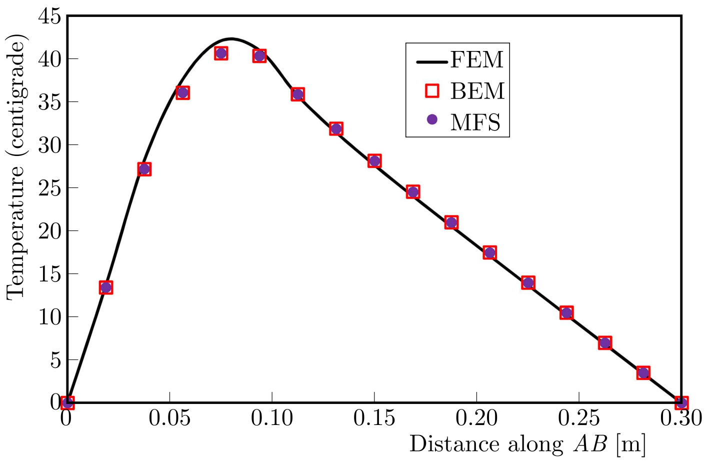

Fig. 7. The FEM, BEM and MFS results for temperature along the line AB of the rectangle with an elliptical heat source

The temperature results along the line AB (Fig. 6a) are depicted in Fig. 7. In this figure, the results based on the presented formulation are compared with those of the BEM (48 linear boundary elements) and FEM (4356 quadratic elements) presented in (Mohammadi *et al.*, 2016). As it can be seen, the presented MFS and the BEM yield accurate results. The computational times (in seconds) for solving this problem using the proposed MFS and the BEM based on

(Mohammadi *et al.*, 2016) have been 2.11 and 6.24, respectively. The reported results indicate that the proposed MFS is more efficient than the BEM for analysis of this example.

4.3. A cubic domain including two circular heat sources with non-uniform intensity

In this example, as shown in Fig. 8, a cube with edges of $L = 10\,\mathrm{m}$, including two circular heat sources, is considered. All faces are kept at $\tau = 0°\mathrm{C}$. The radius of both circular heat sources is $r = 2.5\,\mathrm{m}$.

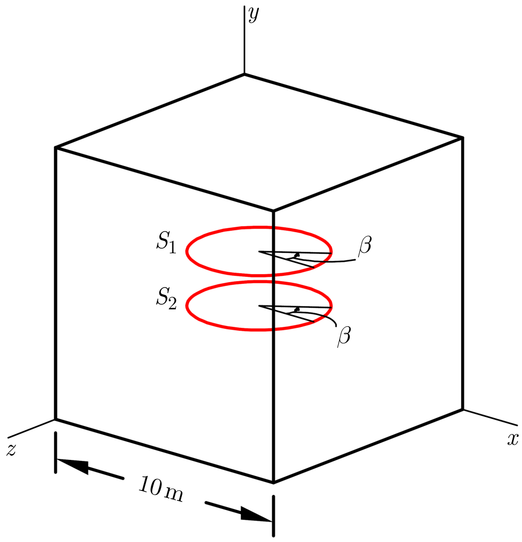

Fig. 8. A cube with two circular heat sources

The first circular heat source is centered at $(5, 6, 5)$ and the second one is centered at $(5, 4, 5)$. The strengths of the sources are considered to be functions of $\beta \in [0, 2\pi]$ with the following forms

$$s_1 = 10000(1 + \cos\beta)\,\mathrm{W/m} \qquad s_2 = 20000(1 + \cos\beta)\,\mathrm{W/m} \tag{4.2}$$

where β is the angular coordinate on the heat sources as shown in Fig. 8.

In the proposed MFS, each circular heat source is modeled by only four quadratic line heat sources. 100 collocation points are considered on each face of the cube. Therefore, 600 collocation points with 600 corresponding source points which are located on the cube with edges of $L' = 14\,\mathrm{m}$ are considered. The configuration of the collocation points and their corresponding source points on a face of the cube is shown in Fig. 9.

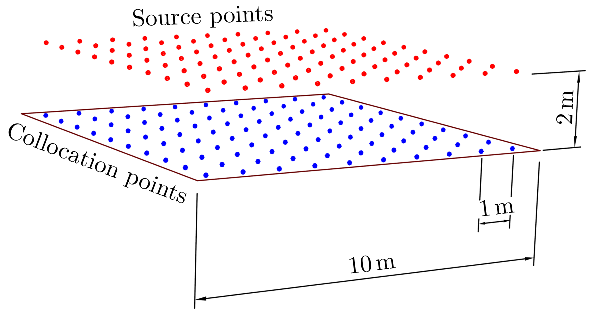

Fig. 9. The configuration of collocation and source points on a face of the cube

The temperature results along the line $x = z = 5$ and the line $x = y = 5$ are shown in Fig. 10. In this figure, the obtained results by the proposed MFS are compared with those of the BEM (600 constant elements) and FEM (56669 3D quadratic elements) presented in

(Mohammadi *et al.*, 2016). As it can be seen, the presented MFS and the BEM formulation yield very accurate results. However, the running CPU time for the BEM is almost 1.8 times the MFS. The computations take 48.1 s for the presented MFS while they take 87.0 s for the BEM.

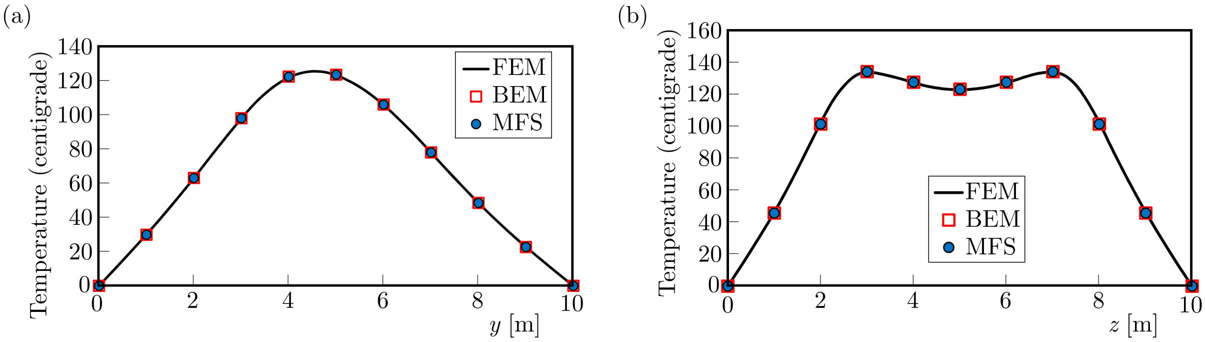

Fig. 10. Temperature on the line (a) $x = z = 5$ and (b) $x = y = 5$ of the cube with circular heat sources obtained by the FEM, BEM and MFS

4.4. A spherical domain including a cylindrical heat source with a non-uniform intensity

In the last example, a spherical domain with the radius $R = 1\,\mathrm{m}$, centered at $(0, 0, 0)$ is considered. The surface of the sphere is kept at $\tau = 0\circ\mathrm{C}$. A surface heat source with a cylindrical shape is included in the domain. The radius, center of the base, and the height of the cylindrical heat source are 0.2 m, $(0, 0, 0)$, and 0.8 m, respectively. A cut-out part of the spherical domain and the cylindrical heat source is shown in Fig. 11a. The intensity per unit area of the source is considered to be a function of $\beta \in [0, 2\pi]$ (angular coordinate on the heat source, measured from the x-axis) and the y-coordinate with the following form

$$s = 20000y(1 + \cos\beta)\ \mathrm{W/m^2} \tag{4.3}$$

In the proposed MFS, the cylindrical heat source is modeled by only eight quadrilateral quadratic heat sources. The pseudo boundary Γ' is considered to be a sphere with the radius $R' = 1.4\,\mathrm{m}$. 98 collocation points and 98 sources are considered for the MFS analysis of the problem. The configuration of collocation and source points are shown in Fig. 11b.

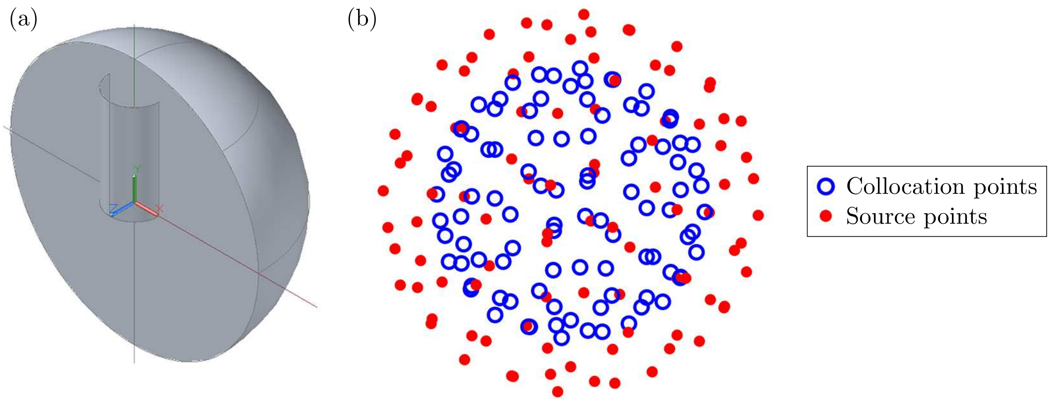

Fig. 11. The spherical domain including a cylindrical heat source: (a) a cut-out part of the domain, (b) the configuration of collocation and source points

So far, this kind of problem has not been solved by the BEM. The obtained results by the presented MFS are compared with those of the FEM. The commercial software package, ANSYS, is employed for the FE analysis. In the FE analysis, the heat source which is concentrated over a cylindrical surface should be modeled as a cylindrical volume with a small thickness. The inner and outer radius of this cylindrical volume are considered as $r_i = 0.18\,\mathrm{m}$ and $r_0 = 0.22\,\mathrm{m}$, respectively. The finite element discretization of the domain with 3D quadratic elements is shown in Fig. 12. The whole domain is discretized with 48 178 elements and 64 869 nodes. In order to visualize the position of the curved surface heat source inside the domain, only a cut-out part of the FE mesh is shown in Fig. 12a. The nodal arrangement of the mesh is depicted in Fig. 12b.

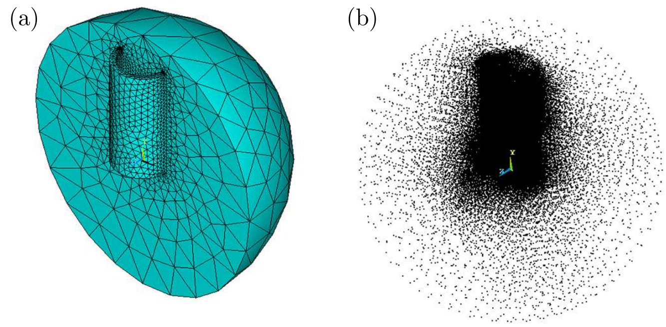

Fig. 12. The finite element discretization of the sphere with a cylindrical heat source: (a) 48 178 elements, (b) 64 869 nodes

The temperature results on the y- and z-axes are depicted in Fig. 13. As it can be observed, the MFS results are in an excellent agreement with the FEM solutions. noteworthy is the fact that the modeling of the problem in the proposed MFS is much simpler than in the FEM.

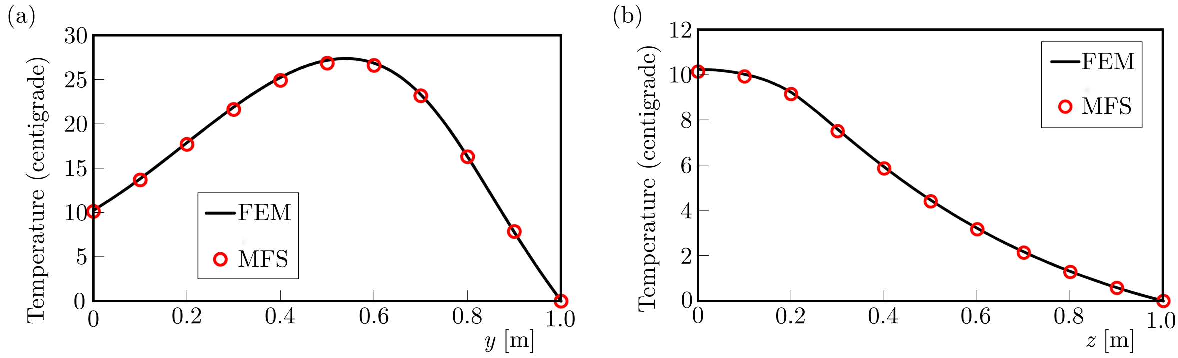

Fig. 13. The FEM, and MFS results for temperature along (a) the y-axis and (b) the z-axis in the sphere with a cylindrical heat source

5. Conclusions

A formulation based on the MFS for analysis of 2D and 3D heat conduction problems in isotropic media containing heat sources concentrated on arbitrary curved lines/surfaces has been presented. The shape and the variation of the intensity of the sources can be arbitrarily and sufficiently complicated.

For 2D problems, curved line heat sources while for 3D problems, curved surface heat sources have been considered. The equations derived for 2D curved line heat sources showed that temperature at points exactly on the source had a finite value. The formulation for 3D curved line heat sources showed that the temperature at points exactly on those sources had an infinite value but the temperature had a finite value at points on the curved surface heat source.

For reliable modeling of a concentrated heat source in the FEM, the source should be modeled as a separated region with a small thickness. Moreover, a large number of internal elements and nodes should also be considered for the modeling of the source. However, these sources can be effectively modeled in the BEM as well as the proposed MFS without considering any internal cells or points. To show the performance of the presented MFS formulation, four numerical examples have been given. It was observed that the proposed method gave accurate results even with a small number of source points and it was found that the computational cost of the presented method was much smaller than the BEM.

Some modified/improved versions of the MFS such as the singular boundary method (Gu *et al.*, 2012) have been presented too. The proposed formulation for the implementation of curved heat sources can be employed for these methods too.

References

1. Ahmadabadi M.N., Arab M., Ghaini F.M., 2009, The method of fundamental solutions for the inverse space-dependent heat source problem, *Engineering Analysis with Boundary Elements*, **33**, 10, 1231-1235
2. Aliabadi M.H., 2002, *The Boundary Element Method, Volume 2, Applications in Solids and Structures*, John Wiley & Sons
3. Atkinson K.E., 1985, The numerical evaluation of particular solutions for Poisson's equation, *IMA Journal of Numerical Analysis*, **5**, 3, 319-338
4. Becker A.A., 1992, *The Boundary Element Method in Engineering: A Complete Course*, McGraw--Hill Book Company
5. Chao C.K., Tan C.J., 2000, On the general solutions for annular problems with a point heat source, *Journal of Applied Mechanical*, **67**, 3, 511-518
6. Fairweather G., Karageorghis A., 1998, The method of fundamental solutions for elliptic boundary value problems, *Advances in Computational Mathematics*, **9**, 1-2, 69-95
7. Golberg M.A., 1995, The method of fundamental solutions for Poisson's equation, *Engineering Analysis with Boundary Elements*, **16**, 3, 205-213
8. Gu Y., Chen W., He X.Q., 2012, Singular boundary method for steady-state heat conduction in three dimensional general anisotropic media, *International Journal of Heat and Mass Transfer*, **55**, 17, 4837-4848
9. Han J.J., Hasebe N., 2002, Green's functions of point heat source in various thermoelastic boundary value problems, *Journal of Thermal Stresses*, **25**, 2, 153-167
10. Hematiyan M.R., Haghighi A., Khosravifard A., 2018, A two-constrained method for appropriate determination of the configuration of source and collocation points in the method of fundamental solutions for 2D Laplace equation, *Advances in Applied Mathematics and Mechanics*, **10**, 3, 554-580
11. Hematiyan M.R., Mohammadi M., Aliabadi M.H., 2011, Boundary element analysis of two- and three-dimensional thermo-elastic problems with various concentrated heat sources, *Journal of Strain Analysis for Engineering Design*, **46**, 3, 227-242
12. Hidayat M.I.P., Ariwahjoedi B., Parman S., Rao, T.V.V.L., 2017, Meshless local B-spline collocation method for two-dimensional heat conduction problems with nonhomogenous and time-dependent heat sources, *Journal of Heat Transfer*, **139**, 7, 071302
13. Karami G., Hematiyan M.R., 2000a, A boundary element method of inverse non-linear heat conduction analysis with point and line heat sources, *International Journal for Numerical Methods in Biomedical Engineering*, **16**, 3, 191-203
14. Karami G., Hematiyan M.R., 2000b, Accurate implementation of line and distributed sources in heat conduction problems by the boundary-element method, *Numerical Heat Transfer, Part B*, **38**, 4, 423-447

15. Kołodziej J.A., Mierzwiczak M., Ciałkowski M., 2010, Application of the method of fundamental solutions and radial basis functions for inverse heat source problem in case of steady-state, *International Communications in Heat and Mass Transfer*, **37**, 2, 121-124
16. Le Niliot C., 1998, The boundary element method for the time varying strength estimation of point heat sources: Application to a two dimensional diffusion system, *Numerical Heat Transfer, Part B*, **33**, 3, 301-321
17. Le Niliot C., Lefèvre F., 2001, Multiple transient point heat sources identification in heat diffusion: Application to numerical two- and three-dimensional problems, *Numerical Heat Transfer, Part B*, **39**, 3, 277-301
18. Mierzwiczak M., Kołodziej J.A., 2012, Application of the method of fundamental solutions with the Laplace transformation for the inverse transient heat source problem, *Journal of Theoretical and Applied Mechanics*, **50**, 4, 1011-1023
19. Mohammadi M., Hematiyan M.R., Khosravifard A., 2016, Boundary element analysis of 2D and 3D thermoelastic problems containing curved line heat sources, *European Journal of Computational Mechanics*, **25**, 1-2, 147-164
20. Partridge P.W., Brebbia C.A., Wrobel, L.C., 1992, *The Dual Reciprocity Boundary Element Method*, Southampton, Computational Mechanics Publications
21. Poullikkas A., Karageorghis A., Georgiou G., 1998, The method of fundamental solutions for inhomogeneous elliptic problems, *Computational Mechanics*, **22**, 1, 100-107
22. Rogowski, B., 2016, Green's function for a multifield material with a heat source, *Journal of Theoretical and Applied Mechanics*, **54**, 3, 743-755
23. Shiah Y.C., Guao T.L., Tan C.L., 2005, Two-dimensional BEM thermoelastic analysis of anisotropic media with concentrated heat sources, *Computer Modeling in Engineering and Sciences*, **7**, 3, 321-338
24. Shiah Y.C., Hwang P.W., Yang R.B., 2006, Heat conduction in multiply adjoined anisotropic media with embedded point heat sources, *Journal of Heat Transfer*, **128**, 2, 207-214
25. Stroud A.H., Secrest D., 1966, *Gaussian Quadrature Formulas*, New York, Prentice-Hall
26. Telles J.C.F., 1987, A self-adaptive coordinate transformation for efficient numerical evaluation of general boundary element integrals, *International Journal for Numerical Methods in Engineering*, **24**, 5, 959-973

Manuscript received December 18, 2017; accepted for print May 8, 2018